

3

Industrial Computational Mechanics

Sophisticated mathematical modelling aided by powerful computing and visualization has the potential to provide the cutting-edge to industry; generation of cost-effective solutions, process optimization and product design are some of the areas where modelling and simulation can play critical to enabling role.

The Industrial Computational Mechanics group at C-MMACS has been utilizing and developing such tools as flow-consistent grid, finite element methods and others to address a wide range of engineering and industrial problems. Several basic results on Finite Element Analyses are reported in this issue.

Inside

Modelling of Smart Structural Systems

Error Analysis for Finite Element Elastostatics and Elastodynamics

Generalization of the Projection Theorem for Finite Element Analysis

3.1 Modelling of Smart Structural Systems

(a) Piezoelectric Finite Element Formulation using Higher Order Theories

The classical theories (beam/plate) do not account for the transverse shear deformation effect and the first order shear deformation theory approximately models the shear effect. However, the transverse shear effects are accurately modelled using higher order shear deformation theories. As the higher order theories do not assume any shear correction factor, they can be applied to both thin and moderately thick laminates. Two higher order theories, namely Lo-Christensen-Wu (LCW) theory and Reddy theory are considered in the present formulation. Both LCW and Reddy theory expand the in-plane displacement fields as cubic functions; however the variation of transverse displacement through the depth is assumed quadratic in the LCW theory and a constant function in Reddy theory.

A beam formulation is made using C^0 continuity for LCW theory and C^1 continuity for Reddy theory. Further a two noded Timoshenko beam element is developed and through static analysis the merit of both the theories is assessed. The beam formulation is being extended to incorporate the electro-mechanical coupling, so that smart piezoelectric composite beam structures can be modelled taking into account the transverse shear effects accurately.

(V Senthilkumar and G Prathap)

(b) Bending Behaviour of Hybrid Actuated Piezoelectric Sandwich Beams

Piezoelectric materials have tremendous potential in vibration control applications as distributed sensors and actuators, which can be either bonded or embedded into composite substrate. However, to effectively use the distributed actuation property (converse piezoelectric coupling), proper modelling techniques and new smart structure concepts must be developed. Such an attempt has been made at C-MMACS by combining shear-bending and extension-bending actuations to develop a piezoelectric hybrid actuation. An orthorhombic crystal system of mm2 class has five piezoelectric constants (d_{31} , d_{32} , d_{33} , d_{15} , d_{24}) and these constants couple the electric field with strain fields. Based on the nature of induced strain, the actuation mechanism may be classified into three types, namely extension-bending actuation (d_{31} , d_{32}), shear bending-actuation (d_{15} , d_{24}) and in-plane actuation (d_{33}).

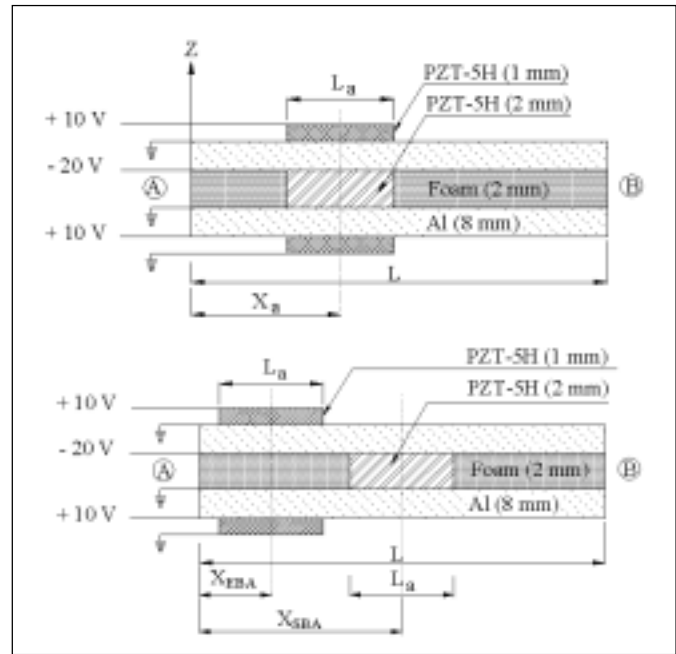


Fig 3.1 Sandwich Beams with Collocated and Non-collocated Actuators

A finite element formulation is developed to analyse the hybrid actuated piezoelectric sandwich beam structures (Fig 3.1). The hybrid actuation is modelled by incorporating a transversely polarized, d_{31} activated extension bending actuation (EBA: full length) lamina and an axially polarized, d_{15} activated shear bending actuation (SBA: full length) lamina (Fig 3.2).

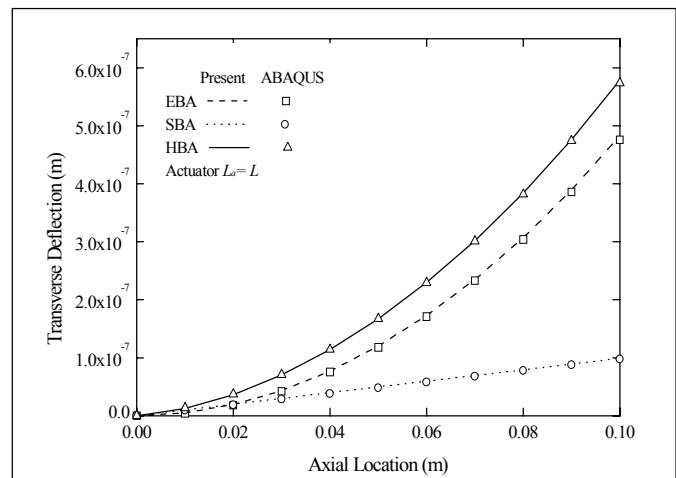


Fig 3.2 Bending Behaviour of Clamped Free (C-F) Sandwich Beams

Further the bending behaviour of sandwich beams are evaluated for various boundary conditions with segmented EBA and SBA (Fig 3.3). The active stiffening effect is assessed through bending deflection behaviour. Also, EBA

and SBA are collocated as well as non-collocated along the length of beam to see the combined actuation effort. It is observed that in the clamped-free case, the actuation effect is augmented with collocated EBA and SBA (Fig 3.4); however this trend is not followed in the other cases. Interestingly, the non-collocated EBA and SBA show better combined actuation effort (Fig 3.4) for different boundary conditions except in hinged-hinged case (Fig 3.5). As EBA and SBA have some distinctive features, both can be employed in a non-collocated fashion for better control action.

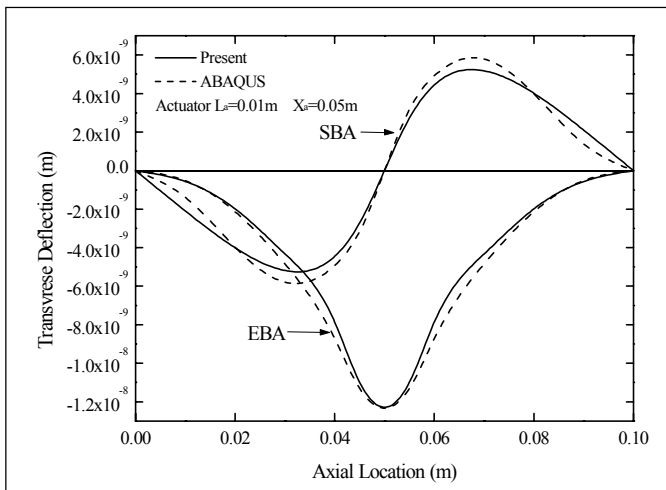


Fig 3.3 Bending Behaviour of Clamped-Clamped (C-C) Sandwich Beams

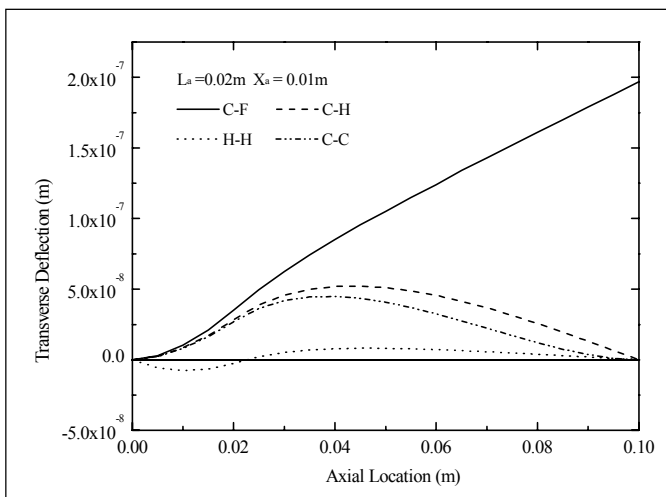


Fig 3.4 Bending Behaviour of Sandwich Beams with Collocated Actuators

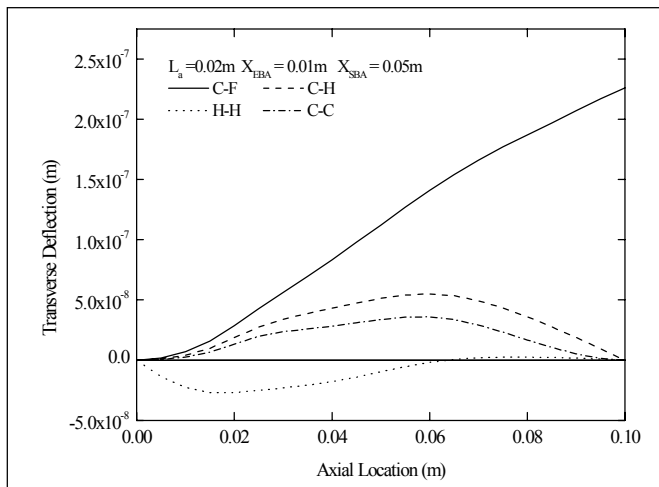


Fig 3.5 Bending Behaviour of Sandwich Beams with Non-Collocated Actuators

(S Raja* and G Prathap)
*NAL, Bangalore

3.2 Error Analysis for Finite Element Elastostatics and Elastodynamics

Finite element analysis is used to solve complex differential equations with varying domain properties and element geometry for which there are no exact solutions. So, it is important to estimate the errors in the approximate solutions in order to ensure the quality of the approximation.

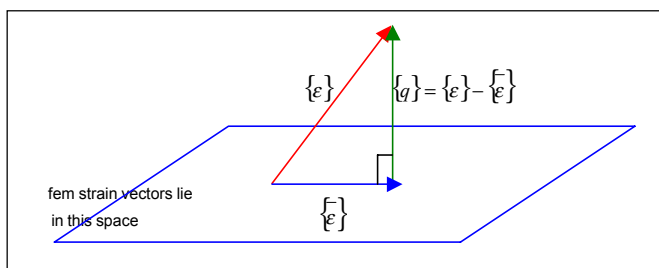


Fig 3.6 A geometric interpretation of the finite element strain vector $\{\bar{\epsilon}\}$ in subspace B , which is closest to the analytical element strain vector $\{\epsilon\}$

Work has been carried out to derive *a priori* estimates of the element strains and errors in finite element elastostatic and elastodynamic analysis. Earlier, studies were carried out for one-dimensional finite element analysis of elastostatic problems with uniform sectional properties. This has now been extended to one-dimensional finite elements with varying sectional properties and also for elastodynamic problems.

3.3 FEA for Elastostatic Problems

Using simple one-dimensional elements with uniform and varying sectional properties, it has been shown with complete mathematical rigor that finite element strains and stresses ($\bar{\epsilon} \bar{\sigma}$) are orthogonal projections of the corresponding analytical elements ($\epsilon \sigma$). The geometric interpretation of finite element analysis for elastostatics is shown in Fig 3.6. The interesting pathological problem of shear locking has been examined using the function space approach. The analysis results are presented graphically in Fig 3.7. Interestingly, both locked and lock-free finite element solutions satisfy the energy error rule for elastostatics.

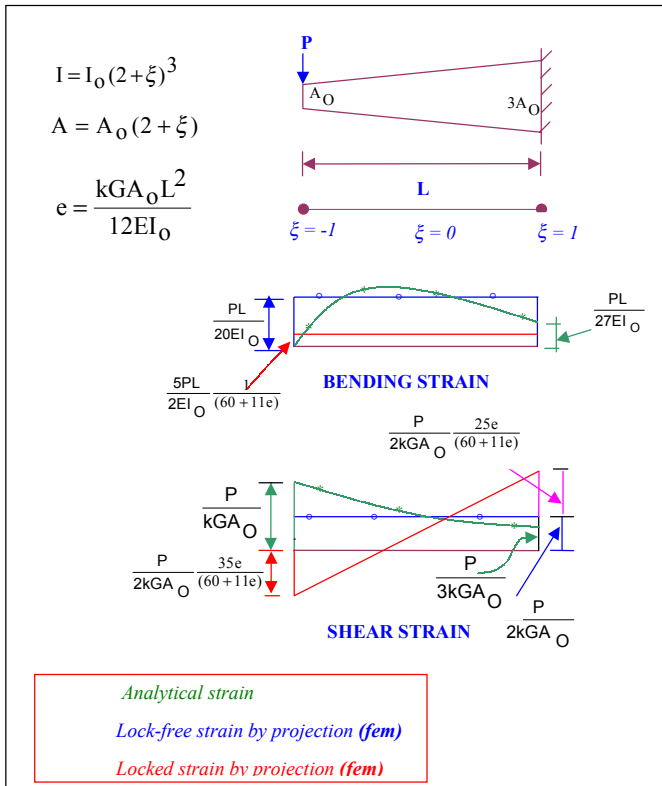


Fig 3.7 Analysis of a cantilever beam with varying sectional properties using a single linear two noded Timoshenko beam element subjected to a point load at the free end

i.e. *strain energy of the error = error in the strain energy*

The rationale behind the practice of using reduced integration for elimination of locking can be revealed explicitly using the rigorous function space approach.

3.4 FEA for Elastodynamic Problems

In finite element analysis literature, there has been no definitive or conclusive work on *a priori* error analysis for elastodynamic problems in general, primarily due to the complex operations involved in the extraction of eigenvalues.

Here we derived the projection theorem for elastodynamics, which states that

$$\begin{aligned} & \text{Total virtual work done by error of stress on approximate strain} \\ & = \text{Total virtual work done by error of inertia force on approximate displacement.} \end{aligned}$$

It is observed that finite element free vibration analysis satisfies the interesting relation

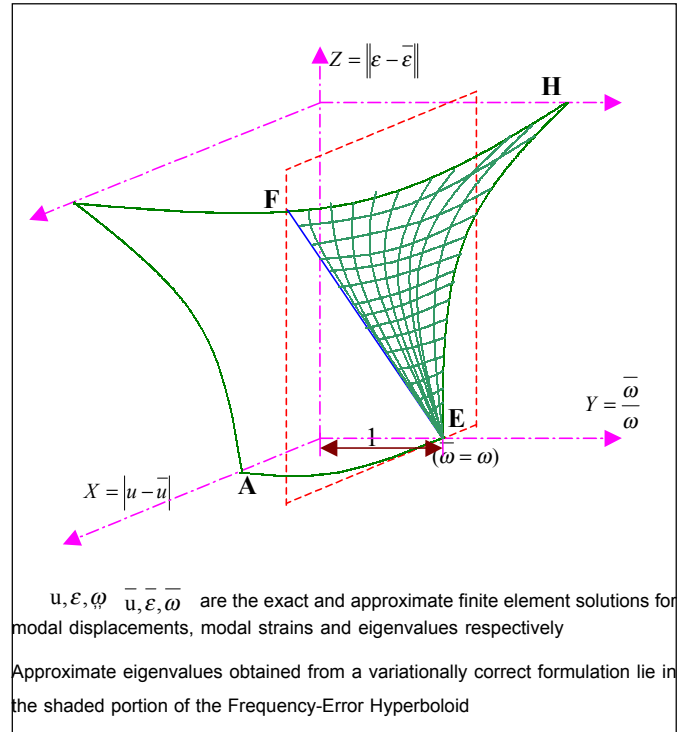


Fig 3.8 Geometric interpretation of eigenvalue analysis of the variationally correct formulation using Frequency-Error Hyperboloid

$$\text{Error of global strain energy} = \text{Error of global kinetic energy.}$$

This can be interpreted as the energy error rule for elastodynamics.

These theories reflect the principle behind the occurrence of errors in free vibration problems. It has been observed that in contrast to elastostatic problems, these theories are valid only at the global level. Furthermore, a geometrical interpretation of the errors associated with the computation of approximate natural frequencies using the Rayleigh Quotient has been derived in terms of a Frequency-Error Hyperboloid (Fig 3.8).

It can be noted that for the ellipse *AE* on the *X-Y* plane and the portion of the hyperboloid connected to it, except for the special point *E*, does not represent any real finite element

computation because of the absurdity of the situation on the X-Y plane that for non-zero values of the displacement error X, all the strain errors Z vanish. Thus the only feasible surface that represents real computational results is that portion of the first octant of the hyperboloid that lies bounded by the straight line EF on one side on the $Y = \bar{\omega} / \omega = 1$ plane, and the hyperbola EH on the other side on the X=0 plane. This shaded portion of the hyperboloid of points representing finite element computation for elastodynamic analysis can be called the Frequency-Error Hyperboloid.

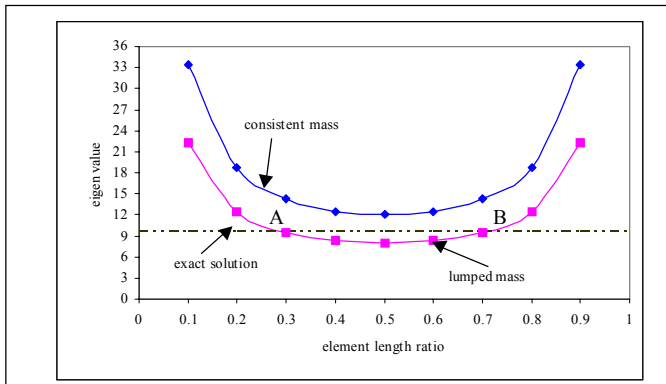


Fig 3.9 Variation of eigenvalue with change in element length (2-element case) for the fundamental mode of a fixed-fixed bar using both consistent and lumped mass

The Frequency-Error Hyperboloid allows us to see geometrically that for arbitrary meshing and for a given mode the approximate values for the eigenvalues computed through variationally correct consistent mass formulations are always higher than the exact values. This is not generally true for the variationally incorrect lumped mass formulations (Fig 3.5). In fact, lumped mass analysis can yield eigenvalues which are either lower than, or higher than, or equal to the exact eigenvalue according to the position of the nodes (Fig 3.9). These predictions have been confirmed with numerical experiments using the one dimensional finite elements.

(P Jafarali, S Mukherjee and G Prathap)
NAL, Bangalore.

3.5 Generalization of the Projection Theorem for Finite Element Analysis

The studies so far on deriving error estimates have been based on the interpretation that the finite element procedure computes element strain and stress which are least squares approximation of the actual state of stress or strain. Such an interpretation also emerges from the projection theorem

of Functional analysis, which shows that the strains computed by the displacement finite element procedure are a best approximation of the true strain at a global level. A closer observation of this best-fit paradigm at an element level reveals that this is valid only if no spurious nodal forces are excited due to the approximation inherent in the discretisation process. This will happen in a class of problems where artificial stiffening takes place due to the discretisation. This violation in the best-fit paradigm at an element level was encountered when finite element method was used to solve the Laplace equation with Dirichlet boundary conditions, and also in case of the Sturm Liouville type differential equation with Dirichlet condition at one end and Neumann condition at the other.

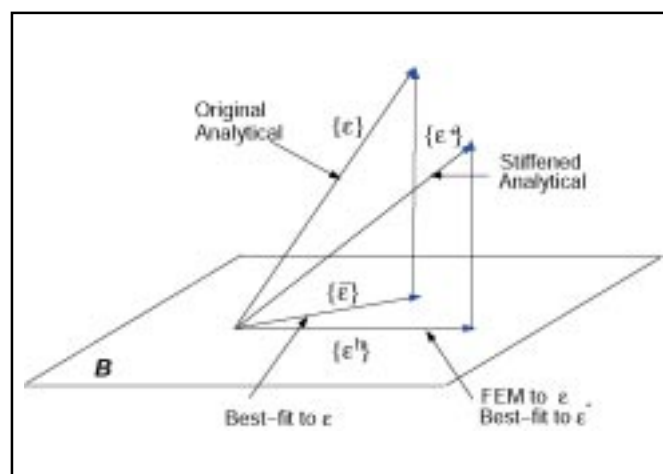


Fig 3.10 Pictorial explanation of the violation of the best-fit paradigm. The FEM solution \mathcal{E}^h in case of stiffened problems is the projection of the analytical solution \mathcal{E}^* of the stiff system

In order to explain this deviation of the finite element solution from the best-fit, a generalization of the projection theorem at an element level has been proposed which states that the best-fit paradigm for finite element analysis remains valid at an element level only if no spurious nodal forces are excited due to the inherent approximation from the discretisation process. For problems with spurious stiffening the FEM solution \mathcal{E}^h is still the best-fit to a modified analytical solution \mathcal{E}^* which takes into account this spurious stiffening effect as shown in Fig 3.10.

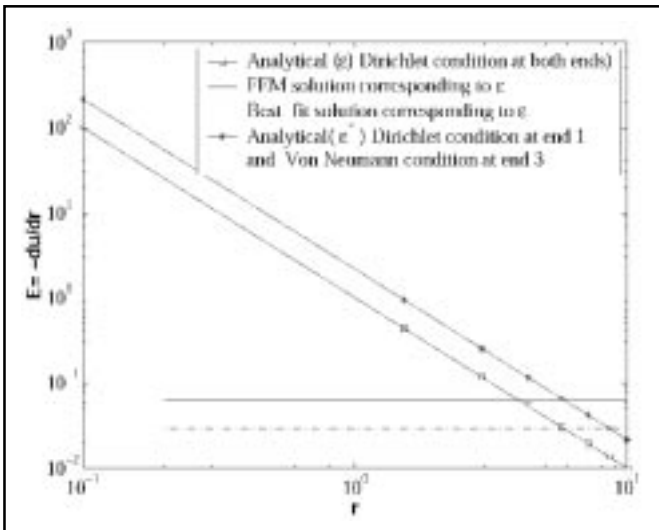


Fig 3.11 Potential gradients obtained by different methods for the Laplace equation with Dirichlet boundary condition at both ends. The FEM solution corresponding to the analytical solution ϵ is the best-fit to ϵ^*

Fig 3.11 validates this theorem for the Laplace equation with Dirichlet boundary condition where it is seen that the FEM solution corresponding to the analytical solution ϵ deviates from the best-fit to ϵ , but is the best-fit approximation to an analytical solution ϵ^* obtained by replacing the Dirichlet condition at one end by the spurious enhanced reaction arising from the discretization of the domain. Results obtained for the Sturm-Liouville problem also validate the generalized projection theorem.

It is concluded that the best-fit paradigm from the original projection theorem which is valid at a global level can also be considered to be valid at an element level if the discretisation process in finite element analysis conserves the nodal reactions.

(K Sangeeta, S Mukherjee and G Prathap)
NAL, Bangalore.